View metadata, citation and similar papers at core.ac.uk

brought to you by CORE

provided by Open Research Online

Open Research Online

The Open University's repository of research publications
and other research outputs

Electron interactions with astro chemical compounds

Journal Item

How to cite:

Thakar, Yogesh; Bhavsar, Rakesh; Swadia, Mohit; Vinodkumar, Minaxi; Mason, Nigel and Limbachiya, Chetan (2019). Electron interactions with astro chemical compounds. Planetary and Space Science, 168 pp. 95–103.

For guidance on citations see FAQs.

© [not recorded]

Version: Accepted Manuscript

Link(s) to article on publisher's website:
http://dx.doi.org/doi:10.1016/j.pss.2019.02.002

Copyright and Moral Rights for the articles on this site are retained by the individual authors and/or other copyright owners. For more information on Open Research Online's data policy on reuse of materials please consult the policies page.

oro.open.ac.uk

Accepted Manuscript

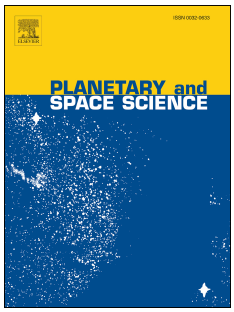

Electron interactions with astro chemical compounds

Yogesh Thakar, Rakesh Bhavsar, Mohit Swadia, Minaxi Vinodkumar, Nigel Mason, Chetan Limbachiya

PII: S0032-0633(18)30189-2

DOI: https://doi.org/10.1016/j.pss.2019.02.002

Reference: PSS 4640

To appear in: *Planetary and Space Science*

Received Date: 12 May 2018

Revised Date: 29 December 2018

Accepted Date: 4 February 2019

Please cite this article as: Thakar, Y., Bhavsar, R., Swadia, M., Vinodkumar, M., Mason, N., Limbachiya, C., Electron interactions with astro chemical compounds, *Planetary and Space Science* (2019), doi: https://doi.org/10.1016/j.pss.2019.02.002.

This is a PDF file of an unedited manuscript that has been accepted for publication. As a service to our customers we are providing this early version of the manuscript. The manuscript will undergo copyediting, typesetting, and review of the resulting proof before it is published in its final form. Please note that during the production process errors may be discovered which could affect the content, and all legal disclaimers that apply to the journal pertain.

ACCEPTED MANUSCRIPT

ELECTRON INTERACTIONS WITH ASTRO CHEMICAL COMPOUNDS

Yogesh Thakar[1], Rakesh Bhavsar[1], Mohit Swadia[2], Minaxi Vinodkumar[3], Nigel Mason[4], Chetan Limbachiya[5]

[1]M. N. College, Visnagar– 384 315, India

[2]H.V.H.P. Institute of P.G. Studies and Research, Kadi-382 715, India

[3]V.P.& R. P. T. P. Science College, VallabhVidyanagar – 388 120, India

[4]The Open University, Milton Keyens, UK

[5,*]The M. S. University of Baroda, Vadodara – 390 001, India

*Email: cglimbachiya-apphy@msubaroda.ac.in

ABSTRACT

In present work electron induced processes with important astro-compounds found in the tholins of Titan are investigated. We report calculated total elastic cross sections Q_{el}, total inelastic cross sections Q_{inel}, total ionization cross sections Q_{ion}, total excitation cross sections $\sum Q_{exc}$ and total cross sections Q_T for hydrogen cyanide (HCN), cyanoacetylene (HCCCN), vinyl cyanide (CH_2CHCN), methanimine (CH_2NH) and ethanimine (CH_3CHNH) on electron impact for energies from ionization threshold to 5keV. We have employed the Spherical Complex Optical Potential (SCOP) formalism to investigate elastic as well as inelastic processes and used Complex Scattering Potential – ionization contribution (CSP-ic) method to derive ionization cross sections. In absence of any theoretical or experimental data of ionization cross sections except for HCN and HCCCN, we have computed Q_{ion} using the Binary- Encounter- Bethe (BEB) method for all these molecules and have found reasonable agreement. This is the maiden attempt to report various total cross sections for all these astro-molecules except HCN and HCCCN.

***Keywords*: Astrochemical compounds; Titan atmosphere; Electron scattering**

INTRODUCTION

The development of modern space based telescopes (e.g Hubble) and large ground based arrays like Atacama Large Millimeter/submillimeter Array (ALMA) has revealed a rich chemical inventory in the interstellar medium, star and planet forming regions as well as various cometary and planetary environments [1]. Such discoveries are fundamental to our exploration of how prebiotic chemistry evolved to develop life on Earth and underpin our investigations of whether life has developed elsewhere. One particularly well studied environment that is believed to provide a mimic for a prebiotic Earth is Titan, the largest satellite of Saturn. Organic chemical reactions in Titan's atmosphere, induced by solar radiation and charged particles including electrons coming from Saturn'smagnetosphere [2, 3] provide a test-bed for prebiotic chemistry.

The dense atmosphere of Titan primarily consists of nitrogen and methane [4]. Cosmic rays, UV radiation coming from the Sun and Saturn's magnetosphere induce electron bombardment that causes dissociation of N_2 and CH_4 leading to complex organic chemistry at higher altitudes on Titan and results in generation of solid aerosols responsible for orange haze surrounding the satellite [5]. Several experiments have been developed to reproduce and study such complex atmospheres in a laboratory [6, 7]. Carrasco and coworkers have developed a plasma device PAMPRE (French acronym for Production d'Aerosolsen Microgravite par Plasma REactifs – Aerosols Production in Microgravity by Reactive Plasma) that has provided significant clues in the understanding of the polymeric chemical structure of the aerosols [8]. The goal of the PAMPRE experiment is to simulate Titan's atmospheric chemistry including the chemical reactivity causing the formation of aerosols, by producing laboratory analogues of these aerosols [6, 9]. A spectrometer aboard the Cassini spacecraft showed formation of tholins in Titan's atmosphere at altitudes greater than 1000 km [5]. The instruments on-board the recently completed Cassini-Huygens mission (NASA/ESA) have exposed new features of Titan's

atmospheric chemistry finding many important molecules, and revealing negative and positive ions in its upper atmosphere [10-14]. Numerical methods are employed to investigate the chemical trail and mechanisms to describe these observations [8, 15-19]. However, such studies (laboratory, observational and modelling) are limited by our poor knowledge of the electron interactions with many of the tholin related compounds. Moreover, electron interactions with molecules of astrochemical interest lead to the chemistry of formation of other compounds and even amino acids which are considered as precursors for life.

In this work we investigate electron interactions with several tholin related compounds and compute the probabilities of occurrence of various electron-driven processes quantitatively through several total cross sections. We have studied hydrogen cyanide (HCN), cyanoacetylene (HCCCN), vinyl cyanide (CH_2CHCN), methanimine (CH_2NH) and ethanimine (CH_3CHNH) all found in the dense tholins of Titan [6, 7]. Methanimine and vinyl cyanide have also been detected in sagattarius-B2 [20, 21] which is a dense interstellar cloud towards the center of the Milky Way. Methanimine is an important molecule in astrobiology since it is an amino acid precursor [22] and when it reacts with hydrogen cyanide, it can form simplest amino acid, glycine. It is protonated imine and is detected in Titan's Ion Neutral Mass Spectrometer (INMS) measurements reinforcing the suspected role of chemical species on aerosol production [7]. Vinyl cyanide is highly flammable and toxic. It is commonly observed in hot cores of interstellar clouds which are sites of formation of massive stars and it has also been detected at lower abundance in cold interstellar clouds [23].

Ethanimine is an organo-nitrogen compound classified as an imine. It is not well known terrestrially but has been detected in abundance towards Sagittarius B2 (Sgr B2) [24]. It is mainly found in hot cores of ISM clouds e,g, in Sgr B2[25]. Cyanoacetylene is a linear polar

molecule found in the upper atmosphere of Titan [6, 7] as well as in the coma of the comet Hale-Bopp [26]. Hydrogen cyanide is the feed gas for the CN laser system [27-29] and has been detected in comets and in the interstellar region [30, 31]. Its dipole moment (2.98 D) is larger than the critical value (1.625 D) at which polar molecule may support bound negative ion states and it is therefore important from fundamental theoretical point of view and hence it is a case study for anion chemistry [32] along with being astro-chemically important [33]. In figure 1 we show schematic diagrams of these molecules.

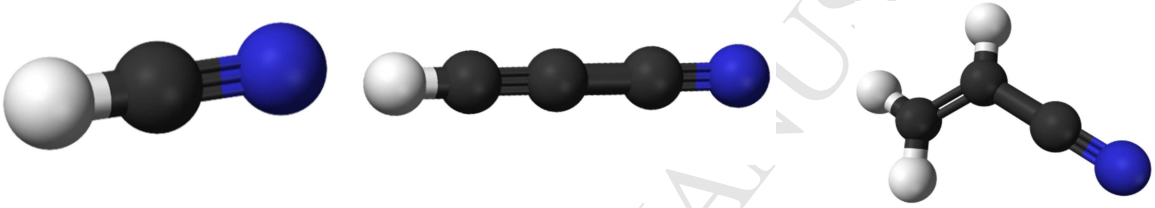

(a) Hydrogen cyanide (HCN)

(b) Cyanoacetylene (HCCCN)

(c) Vinyl cyanide (CH_2CHCN)

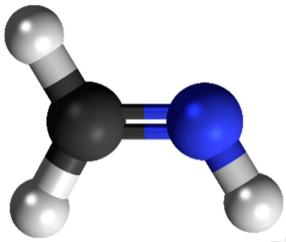

(d) Methanimine (CH_2NH)

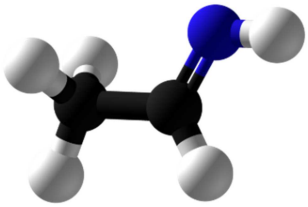

(e) Ethanimine (CH_3CHNH)

Figure 1 schematic diagram of the molecules

[Image courtesy by https://commons.wikimedia.org]

Although, electron interactions with these compounds are important, a literature survey reveals that no electron impact data for these molecules except HCN and HCCCN is reported in the current energy range (ionization threshold to 5000 eV). We present survey of previous study on

electron-driven processes concerning present work along with the range of impact energy in table 1.

In fact, the lack of experimental investigations for these molecules may be ascribed to their toxicity and unavailability in gaseous phase. This motivated us to perform a detailed study of electron interactions with hydrogen cyanide (HCN), cyanoacetylene (HCCCN), vinyl cyanide (CH_2CHCN), methanimine (CH_2NH) and ethanimine (CH_3CHNH) at energies starting from circa ionization threshold (~10 eV) to 5000 eV [34].

Table 1: Previous study on electron impact cross sections

Target	Quantity	Impact energy range (eV)	Reference
Hydrogen cyanide (HCN)	Q_{el}, Q_{inel}, Q_T	Threshold to 5000 eV	Jain and Baluja [35]
		Threshold to 10000 eV	Sanz et al. [36]
	Q_{ion}	Threshold to 5000 eV	Pandya et al. [33]
	Q_T	100 eV to 5000 eV	De Hang et al. [37]
	Q_T	3 eV, 11.6 eV, 21.6 eV and 50 eV	Srivastava et al. [32]
Cyanoacetylene (HCCCN)	Q_{ion}	Threshold to 200 eV	Gilmore and Field [38]
	Q_{ion}, Q_{el}	Threshold to 5000 eV	Kaur et al. [39]
Methanimine (CH_2NH)	Q_{el}	0 to 10 eV	Wang et al. [40]

We have evaluated total cross sections, Q_T, total elastic cross sections, Q_{el} total inelastic cross sections, Q_{inel}, total ionization cross sections, Q_{ion} and summed total excitation cross sections, $\sum Q_{exc}$ for electron interactions with these molecules.

THEORETICAL METHODOLOGY

The present calculations make use of two distinct methodologies, namely the Spherical Complex Optical Potential (SCOP) [41-43] and the Complex Scattering Potential-ionization contribution (CSP-ic) [44, 45], which are appropriate for intermediate to high impact energies (ionization threshold to 5000 eV) to investigate various molecular processes upon interactions with electrons. We present molecular properties which are employed for this computational work in table 2.

Table 2: Properties of target molecules [46]

Molecule	**Ionization Potential (eV)**	**Bond lengths (Å)**	**Polarizability ($Å^3$)**	**Dipole-moment (D)**
Hydrogen cyanide (HCN)	13.60	C–H(1.064),C≡N (1.156)	2.59	2.98
Cyanoacetylene (HCCCN)	11.62	C≡N(1.160),C–C(1.376) C≡C(1.206),C–H(1.062)	5.40	3.72
Vinyl cyanide (CH_2CHCN)	10.91	C–C(1.426), C=C (1.339) C–H(1.086), C≡N (1.164)	8.05	3.87
Methanimine (CH_2NH)	09.97	C=N(1.273), N=H (1.023) C–H(1.081)	2.47	2.00
Ethanimine (CH_3CHNH)	09.50 [47]	C–H(1.087), N–H (1.004) C=N(1.249), C–C (1.499)	5.30	1.90

Spherical complex optical potential (SCOP) formalism

The SCOP method [41-43] exploits the potential scattering formalism to estimate the total probabilities for elastic as well as inelastic processes in terms of total cross sections such that,

$$\boldsymbol{Q_T(E_i) = Q_{el}(E_i) + Q_{inel}(E_i)} \quad (1)$$

where E_i is the incident energy of electrons.

Here $Q_T(E_i)$ represents the sum of all the possible elastic as well as inelastic processes induced by the incident electrons under the spherical approximation.

The potential scattering involves solving of the time independent Schrödinger equation with the complex optical potential corresponding to the electron-molecule system defined as,

$$V_{opt}(r, E_i) = V_R(r, E_i) + i\, V_I(r, E_i) \quad (2)$$

Here $V_R(r, E_i)$ is real and $V_I(r, E_i)$ is an imaginary part of the potential that describe elastic and inelastic interactions respectively. While the real part of the potential comprises of the static potential $V_{st}(r)$, exchange potential $V_{ex}(r, E_i)$ and polarization potential $V_{pol}(r, E_i)$, the imaginary part corresponds to the absorption potential $V_{ab}(r, E_i)$. All these potentials are evaluated by means of spherically averaged molecular charge density $\rho(r)$ computed using the Hartree-Fock wave functions [48].

To describe the electron exchange we used Hara 'Free Electron Gas Exchange' (HFEGE) model [49] given by,

$$V_{ex} = -\frac{2}{\pi} k_F \left(\frac{1}{2} + \frac{1-\eta^2}{4\eta} ln \left|\frac{1+\eta}{1-\eta}\right|\right) \quad (3)$$

Where,

$$\eta = \frac{\sqrt{k^2 + k_F^2 + 2I}}{k_F}$$

Here k is the incident energy of the electrons, k_F is the Fermi wave vector and I is the ionization potential of the molecule under investigation.

While a correlation polarization potential model [50] is employed to describe the polarization effect, all inelastic effects are taken care of by a non-empirical quasi-free absorption potential model [51]

$$V_{abs}(r, E_i) = -\rho(r)\sqrt{\frac{T_{loc}}{2}}\left(\frac{8\pi}{10\, k_F^3 E_i}\right)\ \theta(p^2 - k_F^2 - 2\Delta)(A_1 + A_2 + A_3) \quad (4)$$

The T_{loc} is the local kinetic energy of the incident electrons; k_F is Fermi vector and $\theta(X)$ is the Heaviside unit step-function. The dynamic functions A_1, A_2 and A_3 depend upon the ionization potential I and the energy parameter Δ that decides a threshold below which, $V_{abs}(r, E_i) = 0$, which means ionization and excitation are energetically forbidden [52]. Magnitude of total inelastic cross section is determined through factor Δ [51, 53]. We have modified the original model by considering Δ as a slowly varying function of E_i around I allowing the electronic excitations to occur below the ionization threshold of the target [53, 54] such that,

$$\Delta(E_i) = 0.8I + \beta(E_i - I) \quad (5)$$

For $E_i = I$, we get minimum value of Δ. The second term corresponds to energy dependence of Δ before it attains maximum value I. This energy dependence is governed by parameter β which is determined by imposing the condition $\Delta = I$ at $E_i \geq E_p$. Here E_p is the energy at which we get maximum Q_{inel}.

Complex Scattering Potential – ionization contribution (CSP-ic) technique

In order to estimate the ionization probabilities we use CSP-ic method [52, 55]. We define a dynamic ratio,

$$R(E_i) = \frac{Q_{ion}(E_i)}{Q_{inel}(E_i)} \quad (6)$$

Here $0 < \mathrm{R} \lesssim 1$. The ratio is evaluated using the following conditions,

$$\mathrm{R(E_i)} \begin{cases} = 0 \text{ for } \mathrm{E_i} \leq I \\ = R_p \text{ at } \mathrm{E_i} = \mathrm{E_p} \\ \cong 1 \text{ for } \mathrm{E_i} \gg \mathrm{E_p} \end{cases} \quad (7)$$

Where, R_p is the magnitude of $\mathrm{R(E_i)}$ at $\mathrm{E_i} = \mathrm{E_p}$.

Turner et al. [56] described importance of ionization compared to excitation. They concluded from semi-empirical calculations for gaseous H_2O that if σ_{ion} and σ_{exc} are the cross sections of the ionization and excitation respectively then, above 100 eV [56].

$$\frac{\sigma_{ion}}{\sigma_{ion}+\sigma_{exc}} \approx 0.75 \quad (8)$$

Here, σ_{ion} and Q_{ion} are same but we preserve notations in equation (8) as per reference paper [56].

For many stable molecules like O_2, H_2O, CH_4, etc. experimental ionization cross section are accurately known [53, 57, 58] and it is found that maximum contribution of Q_{ion} to the total inelastic cross sections, Q_{inel} is 70-80%. This tendency is because of the reducing values for $\sum \boldsymbol{Q_{exc}}$ compared to Q_{ion} at higher energies.

The above ratio is determined using the following analytical form [44, 53, 55].

$$\mathrm{R(E_i)} = 1 - \mathrm{C_1}\left(\frac{\mathrm{C_2}}{\mathrm{U+a}} + \frac{\ln(\mathrm{U})}{\mathrm{U}}\right) \quad (9)$$

With $U = \frac{E_i}{I}$.

At higher energies, the ratio $R(E_i)$ tends to unity since Q_{ion} forms major part of inelastic cross sections and the total excitation cross sections $\sum Q_{exc}$ reduce. Moreover the discrete excitation cross sections, mainly due to dipole transitions, reduce as $\frac{\ln(U)}{U}$ at higher energies. The dimension free parameters C_1, C_2 and a depend upon the properties of the target under study and they are evaluated using equation (9). We finally compute Q_{ion} vide equation (6).

We have also calculated Q_{ion} with the help of the Binary-Encounter-Bethe (BEB) method [59]. This well-established method includes the Mott cross sections with the high energy tendency of Bethe cross sections [59]. The BEB model features an analytic relation that uses the energy of incidence, the binding and kinetic energies of the molecule to give the ionisation cross sections with an uncertainty of 10-20% in the non-relativistic description of BEB [59, 60]. Electron-impact ionization of an atom is given by an expression for the cross section of each molecular orbital as:

$$\sigma_{BEB}(t) = \frac{S}{t+u+1}\left[\frac{\ln(t)}{2}\left(1-\frac{1}{t^2}\right)+1-\frac{1}{t}-\frac{\ln(t)}{t+1}\right] \quad (10)$$

Here, $t = {}^{T}/_{B}$, $u = {}^{U}/_{B}$, $S = \frac{4\pi a_0^2 N R^2}{B^2}$, a_0 is the Bohr radius (0.529 Å), R is the Rydberg energy and T is the incident electron energy. N,B and U are the electron occupation number, the binding energy and average kinetic energy of the orbital respectively.

We have calculated Q_{ion} data for the present molecules using BEB formula [61] to offer a comparison with the results of the CSP-ic method [44, 62, 63] which employs various additivity rules. In the CSP-ic method we use group additivity rule [62] to develop molecular charge density from the atomic charge densities. At lower incident energies, the molecular target is treated as a multi-center body and different atomic groups with larger bond lengths can be

treated as separate scattering centers. We define several such groups at the charge density as well as potential level. This treatment is governed by various bond lengths and the atomic number of the constituent atoms. The charge densities of lighter atoms are superimposed on heavier atoms or center of mass depending upon the geometry of the molecule. At high energies the molecule is seen as a single entity.

RESULTS AND DISCUSSION

In this work we have done an exhaustive study of electron interaction with five important astrochemical molecules found in the tholins of Titan, hydrogen cyanide (HCN), cyanoacetylene (HCCCN), vinyl cyanide (CH_2CHCN), methanimine (CH_2NH) and ethanimine (CH_3CHNH).

We present the results along with available comparisons in two categories - **(A) Inelastic cross sections:** In this segment we report graphical results of Q_{inel}, Q_{ion} and $\sum Q_{exc}$. The Q_{ion} are computed using both, the CSP-ic and the BEB method **(B) Elastic cross sections:** In this segment we report the present results on Q_{el} and Q_T.

(A) Inelastic cross sections

Electron driven inelastic cross sections are quantitatively reported through Q_{inel}, Q_{ion} and $\sum Q_{exc}$ in figures 2 to 6 for hydrogen cyanide (HCN), cyanoacetylene (HCCCN), vinyl cyanide (CH_2CHCN), methanimine (CH_2NH) and ethanimine (CH_3CHNH) respectively along with previous data wherever available for energies from ~ionization potential to 5000 eV.

The upper most curves in each of these figures (figure 2 to 6) show present total inelastic cross sections, Q_{inel} that encompasses all the spherical inelastic processes and represents an upper limit for inelastic scattering cross sections. The spherical inelastic processes include only electronic excitation and ionization. In this study we do not consider the non-spherical effects such as

rotations and vibrations of the molecule. Except for HCN, we have not found any data of total inelastic cross sections, Q_{inel} for these molecules. We have also shown the total ionization cross section Q_{ion} in these figures (figure 2 to 6). We have calculated Q_{ion} using two methods, CSP-ic [63] and BEB [59]. All of these results are sensitive to the target geometry, charge density and the ionization potential. In the CSP-ic method we have used the target properties listed in table 1.

The total cross sections, Q_{inel}, Q_{ion} and $\sum Q_{exc}$ for e-HCN are shown in figure 2 along with available comparison. As shown in figure 2, present Q_{inel} data show excellent agreement with the theoretical data of Jain and Baluja [35] across the present energy range. The SCOP theory adopted by Jain and Baluja [35] employs different model potentials to define the electron–molecule interactions. Moreover, they have used a constant Δ=I for the absorption potential in equation (4), which does not allow the discrete excitation processes below the ionization potential. The present Q_{inel} underestimates the results of Sanz et al. [36] significantly. This is due to the Screen Corrected Independent Atom Model (SC-IAM) adopted by Sanz et al. [36], which neglects the molecular bonding and the geometry of the target considered. Here, we have considered bond lengths and geometry of the targets for calculation of molecular charge density from the atomic charge densities [48] using geometrical models [63]. Additionally, Sanz et al. [36] have quoted an uncertainty of 10 -20 % due to interpolation between 30 - 50 eV. Their data merges with the present Q_{inel} above 200 eV since the inelastic cross sections fall as ln (Ei)/Ei at higher energies.

As shown in figure 2 for HCN, the BEB results of Q_{ion} rise rapidly at threshold and are slightly higher compared to the values of Q_{ion} calculated using CSP-ic method particularly at the peak. This behavior at the Q_{ion} (peak) is mainly due to the lower Koopman ionisation potential [64] for

234 HCN. Below 30 eV, present CSP-ic results differ from the BEB results of Pandya et al [33].
235 While the two BEB results show excellent matching, the CSP-ic data of Pandya et al. [33] is
236 shifted leftwards. Pandya et al [33] have studied HCN using different models to develop the
237 molecular charge distribution.

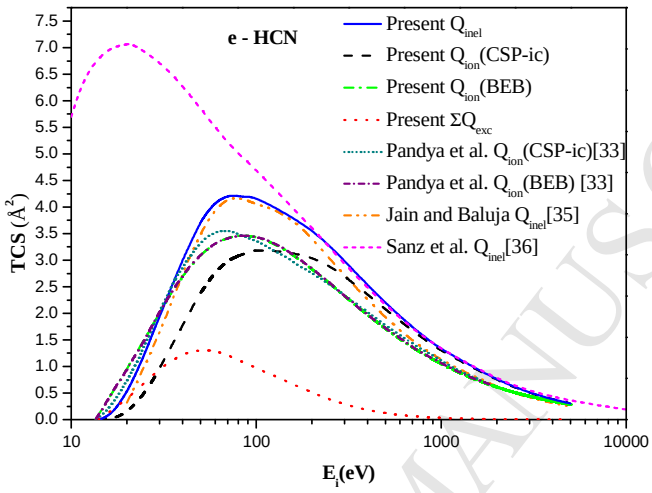

238

239 **Fig. 2 Q_{inel}, Q_{ion} and $\sum Q_{exc}$ for e-HCN scattering**

240 Solid line: Present Q_{inel}; Dash line: Present Q_{ion} (CSP-ic); Dash Dot line: Present Q_{ion} (BEB)
241 Short Dot line: Pandya et al Q_{ion} [33]; Short Dash Dot line: Pandya et al Q_{ion} (BEB) [33];
242 Dash Dot Dot line: Jain and Baluja Q_{inel} [35]; Short Dash line: Sanz et al. Q_{inel} [36]; Dot line:
243 Present $\sum Q_{exc}$

ACCEPTED MANUSCRIPT

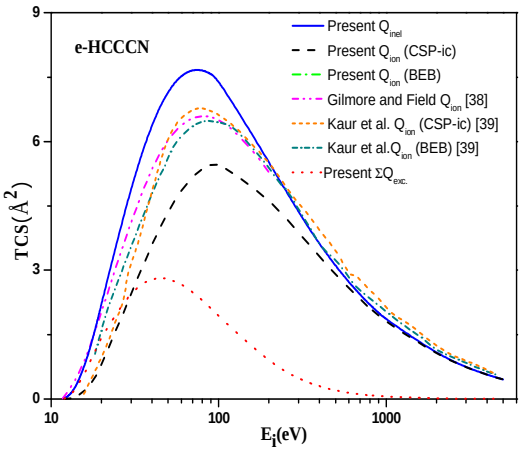

Fig. 3 Q_{inel}, Q_{ion} and $\sum Q_{exc}$ for e-HCCCN scattering

Solid line: Present Q_{inel}; Dash line: Present Q_{ion} (CSP-ic); Dash Dot line: Present Q_{ion} (BEB); Dash Dot Dot : Gilmore Q_{ion} (BEB) [38]; Short Dash :Kaur et al. Q_{ion} (CSP-ic) [39]; Short Dot: Kaur et al. (BEB) [39]; Dot line: Present $\sum Q_{exc}$

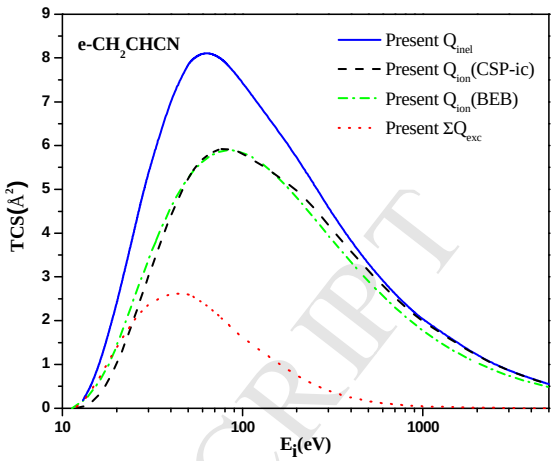

Fig. 4 Q_{inel}, Q_{ion} and $\sum Q_{exc}$ for e-CH_2CHCN scattering

Solid line: Present Q_{inel}; Dash line: Present Q_{ion} (CSP-ic); Dash Dot line: Present Q_{ion} (BEB); Dot line: Present $\sum Q_{exc}$

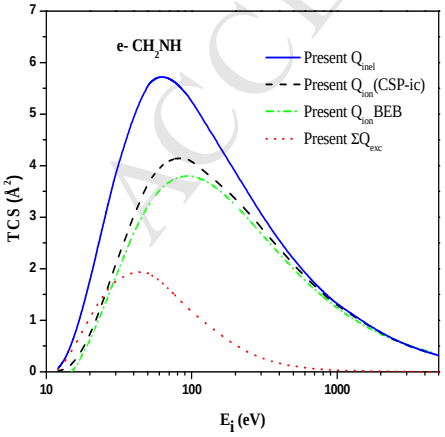

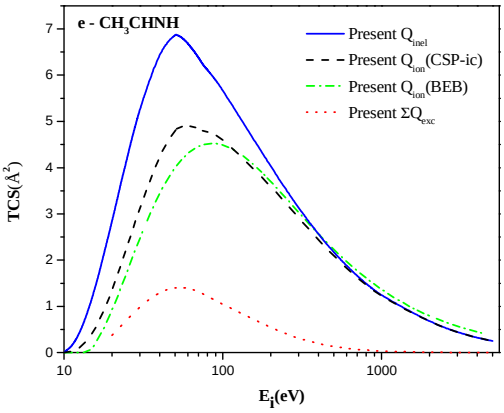

ACCEPTED MANUSCRIPT

Fig 5 Q_{inel}, Q_{ion} and $\sum Q_{exc}$ for e-CH_2NH scattering

Solid line: Present Q_{inel}; Dash line: Present Q_{ion} (CSP-ic); Dash Dot line: Present Q_{ion} (BEB); Dot line: Present $\sum Q_{exc}$

Fig. 6 Q_{inel}, Q_{ion} and $\sum Q_{exc}$ for e-CH_3CHNH scattering

Solid line: Present Q_{inel}; Dash line: Present Q_{ion} (CSP-ic); Dash Dot line: Present Q_{ion} (BEB); Dot line: Present $\sum Q_{exc}$

In figure 3 we have displayed the results of HCCCN and have compared present results of Q_{ion} with the previous BEB data of Gilmor and Field [38] and Kaur et al. [39] as well as CSP-ic data of Kaur et al [39]. The present data underestimate both the previous work [38, 39] but have similar nature of the cross section curve. Differences between the Q_{ion} results obtained through CSP-ic and BEB formalisms are attributed to two aspects (1) In BEB method the ionization potential is computed using the Koopmans theorem [64] and it differs with most experimental ionization potential by about 1 eV. (2) The CSP-ic computation employs various group additivity rules (GAR) [62, 65] to model the charge density as well as the optical potential and Q_{ion} are computed using the dynamic ratio $R(E_i)$ through the parameters C1, C2 and *a* in equation (4). These differences in cross sections are expected since the BEB data are precise within about 10 % accuracy with other measurements and theoretical results [44, 66].

In figure 4, we show present results of e- CH_2CHCN scattering for which no comparison is found in literature. The present Q_{ion} as computed by both the methods show good matching owing to little difference between the ionization potentials used for CSP-ic and the BEB method. The Q_{inel} as well as $\sum Q_{exc}$ rise steadily and attain peak at 64 eV and 50 eV respectively.

The cross sections for methanimine (CH_2NH) and ethanimine (CH_3CHNH) are shown in fig 5 and 6 respectively. For both these cases the Q_{ion} (CSP-ic) attains higher peak value than the Q_{ion}

(BEB) because of the difference in the IP used for the CSP-ic and the Koopman IP used for the BEB computations. The discrete excitation cross sections $\sum Q_{exc}$ and the total inelastic cross sections Q_{inel} are also shown. In table 3 we present the Koopman ionization potential [64] used for BEB calculations along with IP used for CSP-ic method [46, 47]. The influence of ionization potential (IP) on the Q_{ion} is displayed through Q_{ion} (peak) values found for the CSP-ic and BEB calculations in table 3. We also present the computed parameters used in equation (9) and R_p for each molecule for the present study.

Table 3 Values of IP, R_p, Q_{ion}(peak) and parameters C1, C2 and *a*

Molecule	IP (eV)		Parameters			R_p	Q_{ion} (peak) (Å)^2	
	CSP-ic	BEB	C1	C2	a		CSP-ic	BEB
Hydrogen cyanide (HCN)	13.60	13.54	-0.879	-6.938	5.301	0.7	3.21	3.46
Cyanoacetylene (HCCCN)	11.62	13.64	-0.800	-8.104	5.482	0.7	5.50	4.26
Vinyl cyanide (CH_2CHCN)	10.91	11.28	-0.873	-7.015	5.124	0.7	5.92	5.89
Methanimine (CH_2NH)	09.97	14.96	-0.858	-7.202	5.181	0.7	4.14	3.80
Ethanimine (CH_3CHNH)	09.50	13.73	-0.905	-6.656	5.022	0.7	4.90	4.52

As can be seen from table 3, the Koopman IP is somewhat larger than the experimental IP that we used [46, 47] for CSP-ic calculations except for HCN. Therefore the Q_{ion} (peak) (BEB) for all

the molecules is lower than the Q_{ion} (peak) (CSP-ic) except for HCN. In table 3, we have also quoted R_p, the value of $R(E_p)$, which is 0.7 as suggested by Turner et al [56]. The parameters involved in the theory and computation of R_p renders semi-emperical nature to the theory.

In present calculations through CSP-ic method we identify the relative contribution of excitation processes compared with ionization in the form of the summed-total excitation cross-sections $\sum Q_{exc}$. The lower most curves in figure 2 to 6 show present $\sum Q_{exc}$. It is seen that, for all of these targets, the $\sum Q_{exc}$ rises quickly and peaks at around 40 eV before falling rapidly as ln (E) / E for all optically allowed transitions in accordance with the Bethe-Born Approximation [67]. In the literature we do not find any comparison for $\sum Q_{exc}$. Hence, this is the first attempt to report total excitation cross sections for all these astro-molecules.

For ready reference we present the numeric data of the total cross sections, Q_{ion}, Q_{el} and Q_T in table 4 and table 5.

Table 4 Q_{ion}, Q_{el} and Q_T in Å^2 (±10-20 %)

Energy (eV)	Hydrogen cyanide (HCN)			Cyanoacetylene (HCCCN)			Vinyl cyanide (CH_2CHCN)		
	Q_{ion}	Q_{el}	Q_T	Q_{ion}	Q_{el}	Q_T	Q_{ion}	Q_{el}	Q_T
15	0.00	26.20	26.24	0.11	58.05	58.58	0.18	45.99	46.68
20	0.16	21.91	22.45	0.78	51.75	53.97	1.01	39.92	42.31
30	0.93	14.37	16.31	2.43	40.52	45.49	3.01	29.48	34.86
40	1.70	10.54	13.57	3.61	32.40	38.84	4.44	23.61	30.71
80	2.98	5.38	9.59	5.36	17.33	25.00	5.92	15.07	22.97
90	3.06	4.87	9.06	5.46	15.78	23.36	5.89	13.97	21.64
100	3.13	4.48	8.66	5.50	14.63	22.07	5.82	12.98	20.41

600	1.85	1.79	3.73	2.57	4.26	6.98	2.80	4.29	7.20
700	1.67	1.65	3.39	2.32	3.75	6.18	2.53	3.88	6.49
800	1.52	1.54	3.11	2.11	3.36	5.56	2.31	3.58	5.96
900	1.39	1.44	2.88	1.94	3.06	5.06	2.13	3.29	5.47
1000	1.29	1.36	2.68	1.79	2.78	4.63	1.97	3.06	5.08
2000	0.73	0.88	1.62	1.03	1.54	2.60	1.17	1.83	3.01
3000	0.50	0.66	1.17	0.73	1.09	1.83	0.85	1.36	2.22
4000	0.38	0.54	0.92	0.55	0.85	1.41	0.67	1.12	1.79
5000	0.30	0.47	0.77	0.45	0.71	1.17	0.55	0.97	1.52

Table 5 Q_{ion}, Q_{el} and Q_T in Å^2 (±10-20 %)

Energy (eV)	**Methanimine (CH_2NH)**			**Ethanimine (CH_3CHNH)**		
	Q_{ion}	**Q_{el}**	**Q_T**	**Q_{ion}**	**Q_{el}**	**Q_T**
15	0.14	25.65	26.21	0.41	23.23	24.41
20	0.73	19.79	21.57	1.34	20.13	22.97
30	2.07	14.03	17.87	3.12	15.54	20.80
40	3.05	10.79	15.79	4.30	11.88	18.44
80	4.14	5.76	11.34	4.77	6.82	12.94
90	4.14	5.29	10.71	4.71	6.08	11.97
100	4.11	4.91	10.17	4.62	5.52	11.20
600	1.85	1.99	3.91	1.82	1.49	3.37

700	1.66	1.83	3.55	1.62	1.30	2.96
800	1.51	1.70	3.26	1.46	1.16	2.65
900	1.39	1.59	3.02	1.32	1.04	2.39
1000	1.28	1.50	2.81	1.21	0.94	2.18
2000	0.73	0.97	1.71	0.65	0.49	1.15
3000	0.51	0.73	1.25	0.43	0.33	0.77
4000	0.39	0.60	0.99	0.32	0.25	0.57
5000	0.31	0.52	0.83	0.25	0.21	0.46

(B) Elastic cross sections

In this sub section we present our evaluation of the total elastic cross sections Q_{el} and total cross sections Q_T for these astro-molecules. We present our results graphically in figures 7 to 12. To the best of our knowledge there are no previous theoretical or experimental data for Q_{el} or Q_T for these molecules except for HCN and HCCCN.

For HCN we have shown present Q_{el} in figure 7 along with theoretical data of Jain and Baluja [35] and Sanz et al [36]. While present Q_{el} data display overestimation at lower energies, they show very good accord with Jain and Baluja [35] beyond 40 eV and with Sanz et al. [36] beyond 60 eV. Sanz et al [36] have used the screen corrected independent atom model (SC-IAM) that does not include molecular bonding and geometrical effects and is a good tool at higher energies typically beyond 30 eV [36]. We compare our Q_{el} data with the results of Jain and Baluja [35] without the anisotropic term contributions and find reasonable agreement except at lower energies.

In figure 8 we show present Q_T for HCN compared with previous theoretical results [35, 36, 37] and the experimental results of Srivastava et al. [32]. We observe that the present data show reasonable agreement with the results of Sanz et al. [36]. The theoretical data of Jain and Baluja [35] shows good agreement with the present results except at lower energies below 30 eV. This could be attributed to choice of different model potentials by them. For HCN, Srivastava et al. [32] have reported experimental differential cross sections using which, we have obtained Q_T. Srivastava et al. [32] reported measurements of the integral cross sections at 3 eV, 5 eV, 11.6 eV, 21.6 eV and 50 eV. Since the present data do not include non-spherical effects like rotational and vibrational processes we have subtracted the non-spherical cross sections reported by Sanz et al. [36] from integral cross sections of Srivastava et al. [32]. The two derived points with quoted uncertainty of 21 % do not agree with any of the theoretical data. De Heng et al. [37] have reported Q_T from 100 eV-5000 eV. They overestimate the present data up to 500 eV, but thereafter agree with the present data following the Bethe Born trend [67].

In figure 9 we have shown present Q_{el} for HCCCN as compared with the previous Q_{el} data of Kaur et al. [39] along with the present Q_T for which we have not found any experimental or theoretical results in literature. We find large differences for present Q_{el} with the Q_{el} values of Kaur et al [39] below 30 eV, after which the present cross sections show slightly lower values with expected nature of the curve.

ACCEPTED MANUSCRIPT

333

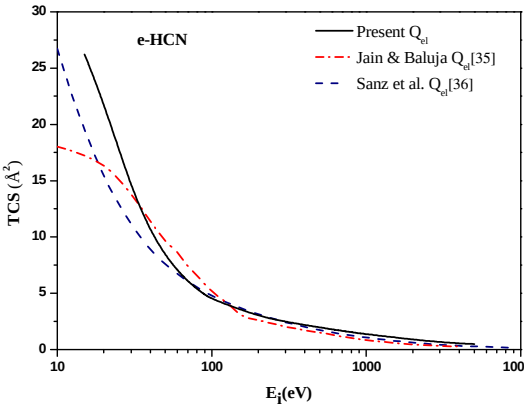

Fig. 7 Q_{el} for e-HCN scattering

Solid line: Present Q_{el}; Dash-Dot line: Jain & Baluja Q_{el} [35]; Short Dash line: Sanz et al. Q_{el} [36]

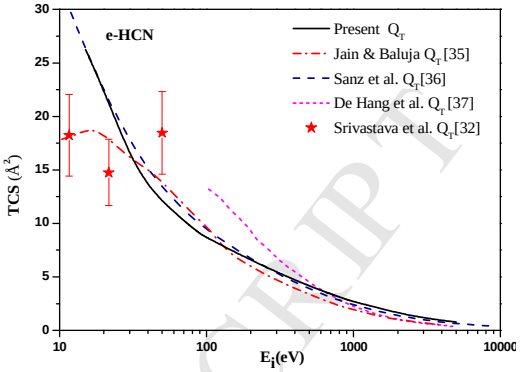

Fig. 8 Q_T for e-HCN scattering

Solid line: Present Q_T; Dash-Dot line: Jain & Baluja Q_T [35]; Dash line: Sanz et al. Q_T [36]; Short Dash line: De-Heng et al.Q_T [37]; Stars:Srivastava et al. Q_T [32]

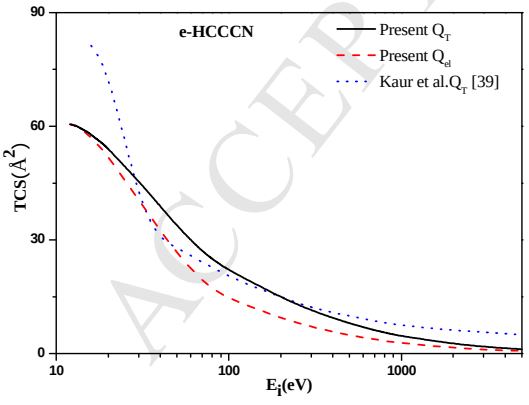

Fig. 9 Q_T and Q_{el} for e-HCCCN

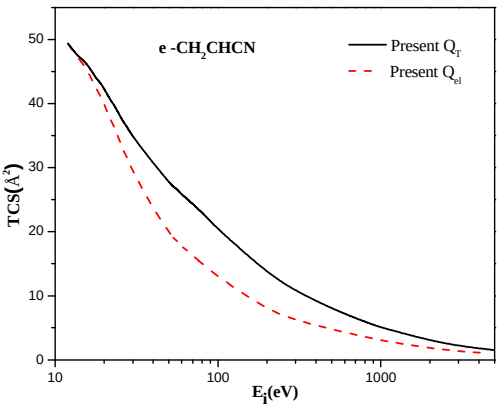

Fig. 10 Q_T and Q_{el} for e-CH_2CHCN

scattering

Solid line: Present Q_T; Dash line: Present Q_{el}; Dash-Dot Dot line: Kaur et al. [39]

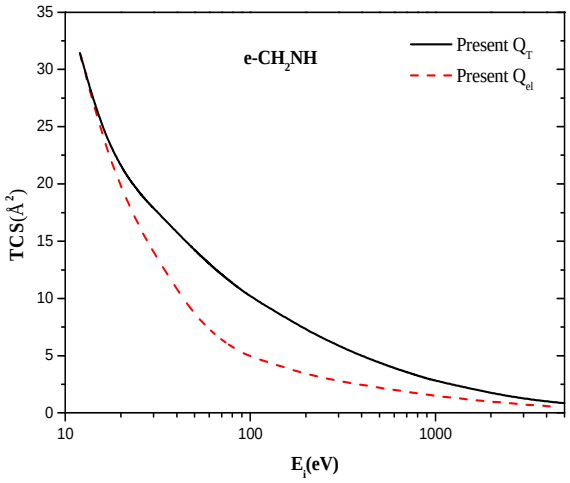

Fig.11 Q_T and Q_{el} for e-CH_2NH scattering

Solid line: Present Q_T; Dash line: Present Q_{el}

scattering

Solid line: Present Q_T; Dash line: Present Q_{el}

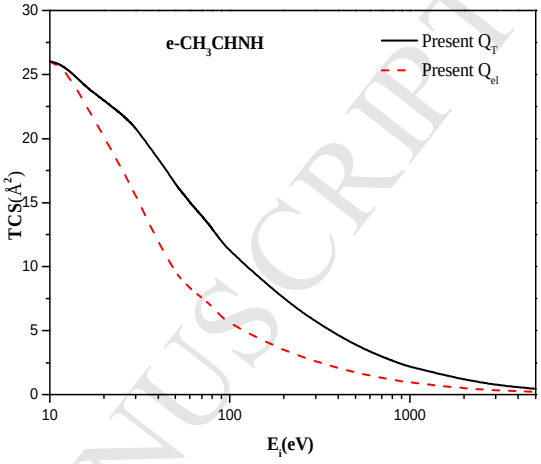

Fig. 12 Q_T and Q_{el} for e-CH_3CHNH scattering

Solid line: Present Q_T; Dash line: Present Q_{el}

In figure 10 we present the Q_{el} and Q_T for e-CH_2CHCN. We do not find any data of Q_{el} or Q_T in literature for this important molecule for comparison with present results in the current energy range. These cross sections values depend on target polarizability, number of electrons and other geometric parameters. Therefore these cross sections reflect the size of the molecule. At the peak

of inelastic cross sections (E_p) the contribution of Q_{el} and Q_{inel} to the total cross sections is 67% and 33% respectively. In figure 11 we show the Q_{el} and Q_T curves for e-CH_2NH scattering. Although, Wang et al. [40] have reported Q_{el} for methanimine, they are at very low energies (0-10 eV) and are not shown here. Q_{el} and Q_{inel} contribute 55% and 45% to Q_T at E_p. The total elastic and total cross sections for e-CH_3CHNH scattering are shown in figure 12. The upper curve shows Q_T and the lower curve Q_{el}. The Q_{el} are sensitive to the polarization potential. While its contribution to Q_T is 58 %, the share of Q_{inel} is 42 % to Q_T at the E_p. The Q_T values show the upper limit of the occurrence of all the e-molecule phenomena in the spherical approximation, a feature further elaborated in figure 13 in terms of relative cross sections.

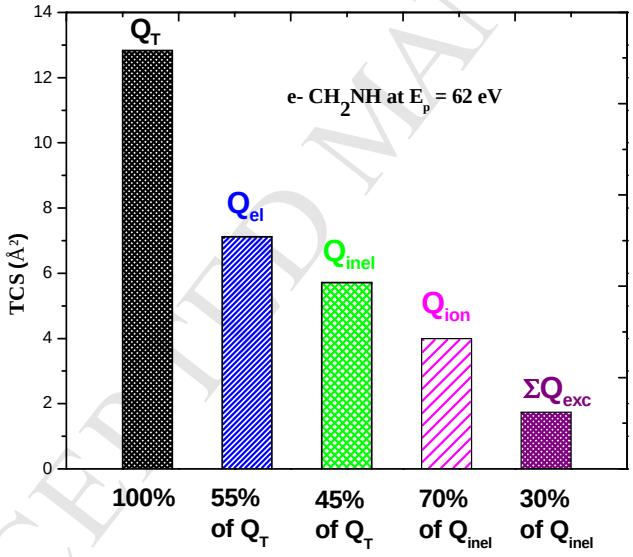

Fig. 13 Contribution of various total cross sections at peak of Q_{inel}

In figure 13 we compare contribution of various total cross sections for e – CH_2NH collision at E_p = 62 eV which is the electron energy for maximum value of Q_{inel}. The total cross sections Q_T cover all the spherical effects induced by electron collision. At the peak of inelastic cross sections the contributions from Q_{el} and Q_{inel} tend to be about equal [68]. In the present case Q_{el} is

353 55% and Q_{inel} is 45% of Q_T at E_p. The total inelastic cross section consists of total ionization and
354 summed total excitation cross sections and the Q_{ion} is about 70% and $\sum Q_{exc}$ is 30% to Q_{inel} at the
355 peak of Q_{inel}. The present methodology provides all these cross sections under the same
356 formalism. This renders consistency to the data.

357

358 **CONCLUSION**

359 We have reported theoretical results on various total cross sections, Q_T, Q_{el}, Q_{inel}, Q_{ion} and $\sum Q_{exc}$
360 for interaction of electrons (~10 eV to 5000 eV) with important astro-molecules, hydrogen
361 cyanide (HCN), cyanoacetylene (HCCCN), vinyl cyanide (CH_2CHCN), methanimine (CH_2NH)
362 and ethanimine (CH_3CHNH), compounds found in dense tholins of Titan. We have employed
363 SCOP to evaluate Q_{el}, Q_{inel} and Q_T and used CSP-ic to compute Q_{ion} and $\sum Q_{exc}$. We have also
364 obtained Q_{ion} using BEB method. Such studies provide a test-bed for prebiotic chemistry that
365 evolved to develop life on Earth. Owing to toxicity and other experimental difficulties, not much
366 previous work is reported for these important astro-compounds. These are the first reports of
367 these cross sections except for HCN and HCCCN in this energy range. For HCN we found good
368 agreement with other earlier data [33, 35] except for the inelastic data of Sanz et al. [36] which
369 significantly overestimates these cross sections at lower energies. The present results of Q_{el} and
370 Q_T for HCN find good accord with the compared theoretical results [35-37] except at lower
371 energies. For HCCCN, while the present Q_{ion} results underestimate the theoretical data [38, 39],
372 present Q_{el} show reasonable matching with Kaur et al [39] beyond 30 eV. The total ionization
373 cross sections Q_{ion} and the peak value Q_{ion} (peak) are sensitive to the ionization potential (table
374 3). For all these compounds summed total excitation cross sections, $\sum Q_{exc}$ are reported for the
375 first time in this work to the best of our knowledge.

Under the spherical approximation, the SCOP and CSP-ic methods are simple, reliable and accurate quantum mechanical methods for study of molecules irrespective of their size, shape and reactivity and provide estimates on various electron driven processes under the same formalism (figure 13). The requirement of spherically symmetric potential due to the use of partial wave analysis that prevents us to include rotational and vibrational effects along with the semi-empirical argument for the value of R_p lead to uncertainty in the cross section values of the order of 10-20 % which is same as quoted in most experimental results. We hope these results will engender other studies, both experimental and theoretical.

Acknowledgement

Minaxi Vinodkumar acknowledges Department of Science and Technology (DST-SERB), New Delhi for financial support through the major research project (EMR/2016/000470).

References

[1] Cordiner, M. A., et al., The Astrophysical Journal Letters **792**, L2 (2014).

[2] Sittler Jr., E.C., et al., Planet. Space Sci. **57 (13)**, 1547–1557 (2009).

[3] Sagan, C. and Thompson, W., ICARUS **59**, 133-161 (1984).

[4] Kuiper, Astrophys. J. **100 (11)**, 378–388 (1944).

[5] Waite, J.H., et al., Science **316**,870–875 (2007).

[6] Gautier T., et al., ICARUS **213**, 625–635 (2011).

[7] Carrasco, N. et al., ICARUS **219**, 230-240 (2012).

[8] Carrasco, N. et al., J. Phys. Chem. A **113 (42)**, 11195–11203 (2009).

[9] Szopa, C., et al., Planet. Space Sci. **54**, 394-404 (2006).

[10] Israel, G., et al., Nature **438 (7069)**, 796–799 (2005).

[11] Hartle, R.E., et al., Planet. Space Sci. **54 (12)**, 1211–1224 (2006).

[12] Yelle, R.V., et al., ICARUS **182 (2)**, 567–576 (2006).

[13] Barnes, J.W., et al., Planet. Space Sci. **57 (14–15)**, 1950–1962 (2009).

[14] Vinatier, S., et al., ICARUS **205 (2)**, 559–570 (2010).

[15] Wilson, E.H., Atreya, S.K., Planet. Space Sci. **51 (14–15)**, 1017–1033 (2003).

[16] Hébrard, E., Dobrijevic, M., Bénilan, Y., Raulin, F., Journal of Photochemistry and Photobiology C: Photochemistry Reviews **C 7 (4)**, 211–230 (2006).

[17] Hébrard, E., Dobrijevic, M., Bénilan, Y., Raulin, F., Planet.Space Sci. **55**, 1470–1489 (2007).

[18] Lavvas, P. P., Coustenis, A., Vardavas, I. M., Planet. Space Sci. **56 (1)**, 67–99 (2008).

[19] Krasnopolsky, V. A., ICARUS **201 (1)**, 226–256 (2009).

[20] Gardner, F. F., Winnewisser, G., Astrophysical Journal **195**, L127-130 (1975).

[21] Godfrey, P. D., et al., Astrophysical Letter **13**, 119-121 (1973).

[22] Marzio, et al., Computational Science and its applications.13thInternational Conference, Vietnam, Conference Proceedings, 47-56 (2013).

[23] William, M. Irvine., Encyclopedia of Astrobiology, springer Berlin Heideberg, 1743-1743 (2011).

[24] Loomis, R. A., et al., The Astrophysical Journal Letters **765,** L9 (2013).

[25] Miao, Y., et al., The Astrophysical Journal Letters **445,** L59 (1995).

[26] Niemann, H. B., et al., Nature **438 (7069),** 779-784 (2005).

[27] Quick, C. R. Jr, Witting, C. and Laudenslager J.B., Opt. Commun., **18**, 268-270 (1976).

[28] West, G. A. and Berry, M.J., J. Chem. Phys. **61**, 4700 (1974).

[29] Korol,V. I. and Kishko, S.M., Opt. Spectroscopy, **38**, 486 (1975).

[30] Whipple, F. L. and Huebner, W. F., Rep. Prog. Phys. **39**, 573 (1976).

[31] Dalgarno, A. and Black, J. H., Rep. Prog. Phys. **39,** 573 (1976).

[32] Srivastava, S. K., Tanaka, H. and Chutjian, A., J. Chem. Phys. **69,** 1493 (1978).

[33] Pandya, S., Shelat, F., Joshipura, K., Vaishnav, B., Int. J. of Mass Spect. **323-324**, 28-33 (2012).

[34] Swadia M., Ph.D. thesis, Kadi Sarva Vishvavidyalaya, India, "theoretical investigations of electrons with molecules of biological and industrial relevance through wide energy range" (2017)

[35] Jain, A. and Baluja, K., Phys. Rev. A **45,** 202 (1992).

[36] Sanz, A. G., et al., J. of Chem. Phys.**137**, 124103 (2012).

[37] De-Heng, S., et al., Phys. Lett. **21(3),** 474-477 (2004).

[38] Gilmore, T.D. and Field, T.A., J. Phys. B: At. Mol. Opt. Phys. **48**, 035201 (2015).

[39] Kaur, J., Mason, N. and Antony, B., J. Phys. B: At. Mol. Opt. Phys. **49**, 225202 (2016).

[40] Wang, K., Meng, J. and Baluja, K. L., Eur. Phys. J. D **69:78**, 1-7 (2015).

[41] Jain, A., Phys. Rev. A **34,** 3707 (1986).

[42] Jain, A., J. Phys. B. **21**, 905-924 (1988).

[43] Limbachiya, C., Vinodkumar, M., Mason, N., Phys. Rev. A **83**, 042708 (2011).

[44] Limbachiya, C., Vinodkumar, M., Swadia, M., Joshipura, K.N. and Mason, N., Molecular Phys. **113(1)**, 55–62 (2015).

[45] Swadia, M., Thakar, Y., Vinodkumar, M., and Limbachiya, C., Eur. Phys. J. D. **71**, 85 (2017).

[46] http://www.cccbdb.nist.gov

[47] Lide, D. R., CRC Handbook of Chemistry and Physics, CRC Press, Boca Raton, FL2005 (1993-1994).

448 [48] Cox, H.L. Jr. and Bonham, R. A., J. Chem. Phys. **47,** 2599 (1967).

449 [49] Hara, S., J. Phys. Soc. Japan **22**,710-718 (1967).

450 [50] Zhang, X., Sun, J. and Liu, Y., J. Phys. B: At. Mol. Opt. Phys. **25**, 1893 (1992).

451 [51] Staszewska, G., Schwenke, D. W., Thirumalai, D. and Truhlar, D .G., Phys. Rev. A **28**,
452 2740 (1983).

453 [52]Vinodkumar, M., Limbachiya, C. and Bhutadia, H., J.Phys. B: At. Mol. Opt. Phys. **43**,
454 015203 (2010).

455 [53] Vinodkumar, M., Limbachiya, C., Antony, B. and Joshipura, K. N., J. Phys. B: At. Mol.
456 Opt. Phys. **40**, 3259 (2007).

457 [54] Vinodkumar, M., Limbachiya, C., Joshipura, K., Vaishnav, B., Gangopadhyay, S., Journal
458 of Physics: Conference Series, **115,** 012013 (2008).

459 [55] Rahman, M., Gangopadhyay, S., Limbachiya, C., Joshipura, K., Krishnakumar, E., Int. J.
460 Mass Spectrom. **319–320**, 48-54 (2012).

461 [56] Turner, J. E., Paretzke, H. G., Hamm, R. N., Wright H. A. and Richie, R. H., Radiation
462 Research: **92(1)**, 47-60 (1982).

463 [57] Blanco, F. and Garcia, G., Phys. Lett. A **317**, 458-462 (2003).

464 [58] Karwasz, G. P., Brusa, R. S. and Zecca, A., RIV NUOV CI **24(4)**,1-101 (2001).

465 [59] Kim, Y., and Rudd, M., Phys. Rev. A **50**, 3954 (1994).

466 [60] Kim, Y., and Desclaux, J., Phys. Rev. A **66**, 012708 (2002).

467 [61] Kim, Y., and Stone, P., Phys. Rev. A **64**, 052707 (2001).

468 [62] Vinodkumar, M.,Limbachiya, C.,Barot, M., Swadia, M., Barot, A. , Int. J. of Mass
469 Spectrom. **339-340**, 16-23 (2013).

470 [63] Joshipura ,K., Vinodkumar, M.,Limbachiya, C., and Antony, B., Phys. Rev. A **69**, 022705
471 (2004).

ACCEPTED MANUSCRIPT

472 [64] Koopmans, T., Physica **1**,104 (1933).

473 [65] Vinodkumar, M., Limbachiya, C., Joshipura, K., and Mason, N., Eur. Phys. J. D **61**,579-585

474 (2011).

475 [66] Limbachiya, C., Vinodkumar, M., Swadia, M. and Barot A., Molecular Physics **112(1)**,

476 101–106 (2014).

477 [67] Schram, B.L. and Vriens, L., Physica **31**, 1431-1436 (1965).

478 [68] Joachain, C.J., Quantum Collision Theory (Amsterdam: North-Holland), 107 (1983).

ACCEPTED MANUSCRIPT

ACCEPTED MANUSCRIPT

Highlights

Article reference: PSS_2018_133

Title: ELECTRON INTERACTIONS WITH ASTRO CHEMICAL COMPOUNDS

Yogesh Thakar, Rakesh Bhavsar, Mohit Swadia, Minaxi Vinodkumar, Nigel Mason, Chetan Limbachiya

- The paper deals with theoretical study of various electron induced phenomena for important astrochemical molecules which are relevant for chemistry in the tholins of Titan, the largest satellite of Saturn.

- The theoretical methods employed for this study are:
  (1) Spherical Complex Optical Potential (SCOP) method
  (2) Complex Scattering Potential-ionisation contribution (CSP-ic) method
  (3) Binary-Encounter-Bethe (BEB) method

- Computed total cross sections on electron impact with hydrogen cyanide (HCN), cyanoacetylene (HCCCN), vinyl cyanide (CH_2CHCN), methanimine (CH_2NH) and ethanimine (CH_3CHNH) are reported for energies ~10 eV to 5000 eV, along with comparison wherever available.

- The reported electron impact total cross sections are total elastic cross sections Q_{el}, total inelastic cross sections Q_{inel}, total ionization cross sections Q_{ion}, total excitation cross sections $\sum Q_{exc}$ and total cross sections Q_T.

- We have employed SCOP to evaluate Q_{el}, Q_{inel} and Q_T and used CSP-ic to compute Q_{ion} and $\sum Q_{exc}$. We have also obtained Q_{ion} using the BEB method.

ACCEPTED MANUSCRIPT